Muon-spin relaxation and heat capacity measurements on the magnetoelectric and multiferroic pyroxenes $LiFeSi_2O_6$ and $NaFeSi_2O_6$

P. J. Baker,[1,2,*] H. J. Lewtas,[1] S. J. Blundell,[1] T. Lancaster,[1] I. Franke,[1] W. Hayes,[1] F. L. Pratt,[2] L. Bohatý,[3] and P. Becker[3]

[1]*Department of Physics, Clarendon Laboratory, Oxford University, Parks Road, Oxford OX1 3PU, United Kingdom*

[2]*ISIS Pulsed Neutron and Muon Source, STFC Rutherford Appleton Laboratory, Harwell Science and Innovation Campus, Didcot, Oxfordshire OX11 0QX, United Kingdom*

[3]*Institut für Kristallographie, Universität zu Köln, Zülpicher Straße 49 b, 50674 Köln, Germany*

(Received 8 February 2010; revised manuscript received 5 May 2010; published 3 June 2010)

We present the results of muon-spin relaxation and heat capacity measurements on $LiFeSi_2O_6$ and $NaFeSi_2O_6$. In synthetic samples of both compounds we see a single muon oscillation frequency consistent with commensurate magnetic structures below T_N. In contrast, for a specimen of naturally occurring $NaFeSi_2O_6$, in which multiferroicity has been observed, a rapid Gaussian depolarization of the muon polarization is observed instead, showing that the magnetic structure in this case is more complex. Heat capacity measurements reproduce the phase diagrams previously derived from other techniques and demonstrate that the main contribution to the magnetic entropy is associated with the buildup of correlations in the quasi-one-dimensional Fe^{3+} chains.

DOI: 10.1103/PhysRevB.81.214403 PACS number(s): 76.75.+i, 75.50.Ee, 75.85.+t

I. INTRODUCTION

Multiferroic materials demonstrating coupled magnetic and ferroelectric order have once again become an active field of research since they offer both interesting physical properties and the possibility of technological applications.[1–3] While an increasing number of multiferroic materials have been discovered in recent years[4–7] and much progress has been made in finding general rules to describe the origins of this effect[8,9] it is not always possible to predict if a given material will be multiferroic. Isostructural series have already provided considerable insights into multiferroicity, notable examples being the hexagonal and orthorhombic manganites.[10,11] Competing magnetic interactions and a strong magnetoelastic coupling are both known to favor multiferroicity. In this context the discoveries of multiferroicity in the pyroxene compound $NaFeSi_2O_6$ and magnetoelectricity in $LiFeSi_2O_6$ have suggested that this geologically common family may offer more multiferroic compounds, as well as providing an opportunity to study isostructural materials with different spins and magnetic exchange constants.[12]

Pyroxene compounds have chemical formulas $A^+M^{3+}(Si,Ge)_2O_6$ and chains of M^{3+} ions surrounded by oxygen octahedra lie along the crystallographic c axis.[13] The M^{3+} chains are connected by $(Si,Ge)O_4$ tetrahedra. This structure is shown in Fig. 1. Most magnetic members of this family show Néel ordering at low temperature, a notable exception being the orbitally assisted spin-Peierls transition seen in $NaTiSi_2O_6$.[14,15] Common to both the Néel ordered and spin-gapped compounds is the dominant intrachain exchange interaction giving quasi-one-dimensional magnetic properties.

$LiFeSi_2O_6$ has a Néel temperature of 18 K and there is no pyroelectric current without an applied magnetic field.[12] Applying a magnetic field along the c axis reduces the temperature of the peak of the magnetic susceptibility to 14 K at 14 T and measurements of the pyroelectric current, I_b, show a peak which follows the same magnetic field dependence as that in the magnetic susceptibility. Smaller peaks in I_b at higher temperature were also observed but their origin is unclear.[12] The magnetic structure has been determined to be antiferromagnetically coupled ferromagnetic chains with magnetic space group $P2_1/c'$.[16] This allows for magnetoelectric effects consistent with those observed. The isostructural compound $LiCrSi_2O_6$ was found to have comparable magnetic and magnetoelectric properties.[12,17]

The situation in $NaFeSi_2O_6$ is rather more complex, largely because of the differences observed between natural and synthetic samples. Natural samples, which are known to contain impurities, show two phase transitions in zero magnetic field: ordering at 8 K, then entering a ferroelectric ($P \| b$) phase at 6 K. In fields above 4 T a ferroelectric ($P \| c$) phase was observed below 5 K.[12] Synthetic samples showed a similar magnetic structure to $LiFeSi_2O_6$, albeit with evidence for a further incommensurate modulation to this structure that could not be determined.[18] Very recently the magnetoelectric and toroidic effects in $NaFeSi_2O_6$ have been analyzed theoretically, showing that the antiferromagnetic-

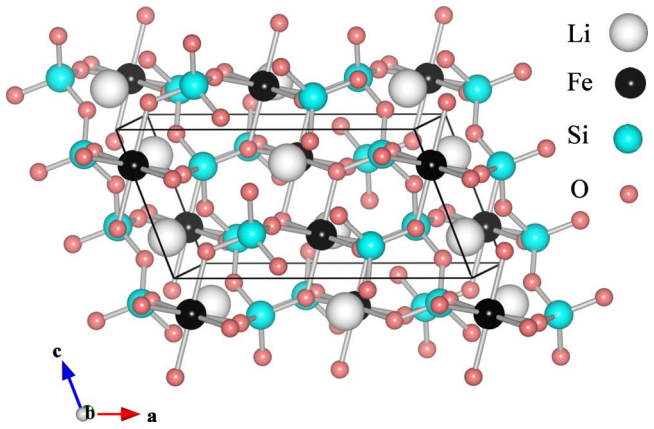

FIG. 1. (Color online) Structure of $LiFeSi_2O_6$ showing the Fe^{3+} chains running along the c axis linked by SiO_4 tetrahedra. The structural data come from Ref. 16.

ferroelectric phase is induced by replication of a single transition order parameter, the first example of such an effect to be identified.[19]

Detailed *ab initio* calculations for a broad range of pyroxene compounds were carried out by Streltsov and Khomskii.[20] They modeled the exchange constants in terms of an intrachain exchange J, and two interchain exchange constants, J_1 and J_2, all of which were found to be antiferromagnetic for both compounds. The calculations suggest J^{Li}=7 K, J_1^{Li}=1.9 K, and J_2^{Li}=3.4 K; and J^{Na}=8.5 K, J_1^{Na}=0.8 K, and J_2^{Na}=1.6 K.[20] These values suggest that the magnetism in $LiFeSi_2O_6$ is likely to be more three dimensional than that in $NaFeSi_2O_6$ and the different exchange constants may have an even more significant effect on the fine details of the magnetic structure and any magnetostriction.

In this paper we investigate synthetic samples of the two pyroxene compounds $LiFeSi_2O_6$ and $NaFeSi_2O_6$, and a natural sample of $NaFeSi_2O_6$, using heat capacity and muon-spin relaxation (μSR) measurements. These probe the change in magnetic entropy around the phase transitions and the local magnetic field distributions within the samples. While there are some underlying similarities in the magnetic properties, the effects of the changing exchange constants and the presence of impurity-induced disorder in the natural sample are clearly evident in the data recorded by both techniques.

II. EXPERIMENTAL

A. Samples

Our natural sample of $NaFeSi_2O_6$ was cut from the same crystal that was used in Ref. 12. Electron microprobe analysis has shown that the composition is $Na_{1.04}Fe_{0.83}Ca_{0.04}Mn_{0.02}Al_{0.01}Ti_{0.08}Si_2O_6$.[12] The synthetic sample of $LiFeSi_2O_6$ was composed of small translucent single crystals grown from melt solution (see also Ref. 12). The powder sample of synthetic $NaFeSi_2O_6$ was obtained by crystallization of glassy $NaFeSi_2O_6$ that was prepared using high-temperature flux.

B. Heat capacity measurements

Heat capacity measurements were made using a Quantum Design Physical Properties Measurement System (PPMS) in magnetic fields between 0 and 10 T. Data for the three samples are presented in Fig. 2. They show clear peaks associated with the magnetic ordering transitions found using other techniques[12] and a broad hump above T_N due to the buildup of correlations in the chains. Some information about the dimensionality of the system can be obtained from the form of the hump and the relative size of the peak.[21] The lattice contribution for each compound was modeled using one Debye and two Einstein components, compatible with both the two optic modes found around 300 and 700 K by Raman scattering[22] and the Dulong-Petit limit at high temperature. Parameters derived from fits of the data above 50 K are given in Table I together with the magnetic entropy (S_{mag}) extracted from the difference between the data and the lattice model below 50 K. The agreement of the Einstein

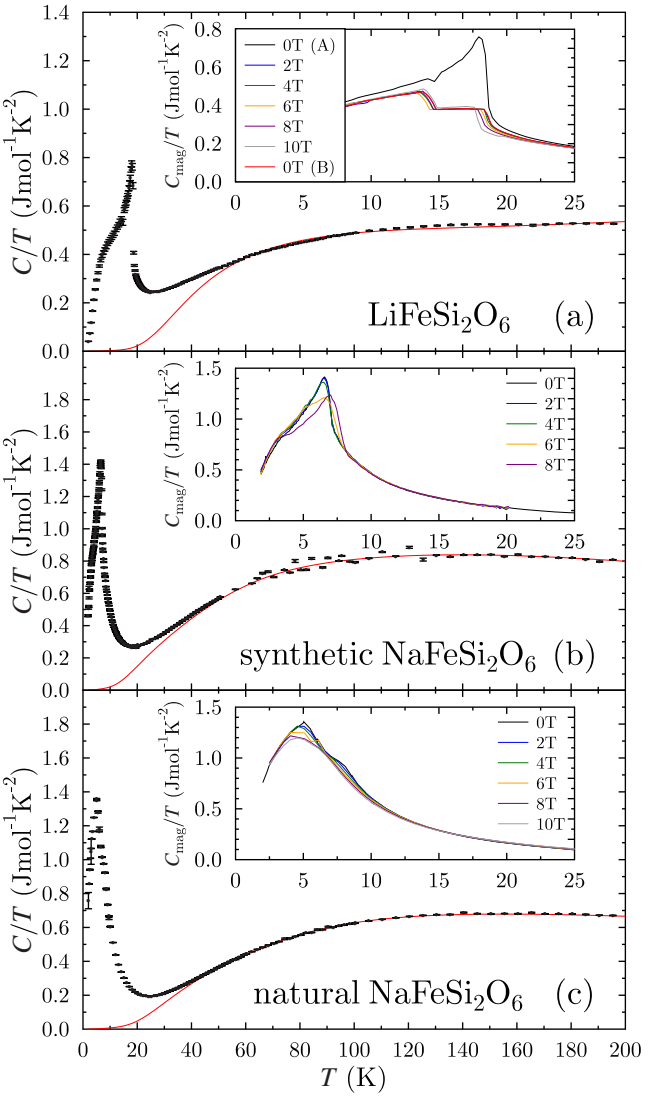

FIG. 2. (Color online) Heat capacity measurements on (a) $LiFeSi_2O_6$, (b) synthetic $NaFeSi_2O_6$, and (c) natural $NaFeSi_2O_6$. The lines in the main panels show the fitted lattice terms described in the text and the insets show the variation with applied magnetic field close to the magnetic ordering transitions described in the text.

modes with the optical data[22] is adequate since the acoustic mode and any anharmonicity present in the system will affect the fitting. We would expect a magnetic entropy of S_{mag}=14.9 J mol^{-1} K^{-1} for the S=5/2 Fe^{3+} ions in these

TABLE I. Parameters derived from fitting the heat capacity data as described in the text. The magnetic entropy S_{mag} is evaluated up to 50 K.

Sample	$LiFeSi_2O_6$ synthetic	$NaFeSi_2O_6$ synthetic	$NaFeSi_2O_6$ natural
θ_D (K)	621(18)	370(20)	530(20)
θ_{E1} (K)	192(3)	190(10)	165(5)
θ_{E2} (K)	1210(50)	700(50)	1050(50)
S_{mag} (J mol^{-1} K^{-1})	11.2	11.2	13.9

samples but in each the observed value is smaller. This could be because the approximation to the lattice contribution is not ideal or the Fe^{3+} ions do not have their full effective spin at low temperature.

In zero applied field the three samples show the buildup of short-ranged correlations in the chains from well above T_N. In $LiFeSi_2O_6$ this corresponds to around 80% of the magnetic entropy, in synthetic $NaFeSi_2O_6$ around 65%, and in the natural $NaFeSi_2O_6$ about 90%. Our data for synthetic $NaFeSi_2O_6$ are in quantitative agreement with those of Ko *et al.*[23] From the shapes of the hump due to short-ranged order in each sample we can estimate[21] intrachain exchange constants ($J^{Li} \sim 7$ K, $J^{Na} \sim 6.5$ K) roughly consistent with the calculations of Streltsov and Khomskii,[20] though the comparison is complicated significantly by the interchain exchange.

In applied magnetic field the heat capacity of $LiFeSi_2O_6$ shows an unusual hysteresis. On warming, the data closely follow the zero-field data [0 T (A)] but on cooling from around $2 \times T_N$ in the measurement field two steps are evident, accompanied by small amounts of latent heat (evident in the poorer fits to the raw thermal relaxation data recorded by the PPMS) and persist down to zero applied field [0 T (B)]. This behavior suggests that short-range order persists well above T_N and produces hysteresis in the sample when fields are applied. From the heat capacity measurements we cannot draw direct conclusions on the nature of the magnetism in these field-induced states. Neutron-scattering measurements on $LiFeSi_2O_6$ in applied field would therefore be worthwhile, particularly if a comparison with the behavior in natural $NaFeSi_2O_6$ could be made.

C. μSR measurements

Our positive μSR measurements[24] ($\tau_\mu = 2.2$ μs and $\gamma_\mu = 2\pi \times 135.5$ MHz T^{-1}) were carried out on the General Purpose Surface-Muon Instrument at the Paul Scherrer Institute, Switzerland. The muon spins are sensitive to both static and fluctuating local magnetic fields at their stopping positions inside the material, and these affect the time dependence of the muon decay asymmetry, $A(t)$. Data were analyzed using the WiMDA program.[25] In the paramagnetic phase of each compound the muon relaxation is well described by a single exponential relaxation. For $LiFeSi_2O_6$ and synthetic $NaFeSi_2O_6$ [Figs. 3(a) and 3(b)] we observe coherent muon precession below T_N consistent with long-range magnetic order and quasistatic magnetic fields at the muon stopping site. The data are well described by

$$A(t) = A_1 e^{-\lambda_1 t} \cos(2\pi\nu t) + A_2 e^{-\lambda_2 t}. \quad (1)$$

The first term describes damped muon precession around quasistatic local fields ($B = 2\pi\nu/\gamma_\mu$) perpendicular to the muon-spin polarization and the second term is an exponential relaxation, of rate λ_2, due to fluctuations flipping the spins of muons having a nonzero spin component along the local magnetic field direction. We find that the ratio $A_1/A_2 \sim 2$, which is consistent with polycrystalline averaging for long-range magnetic order throughout the samples. In $LiFeSi_2O_6$ λ_1 and λ_2 are almost temperature independent.

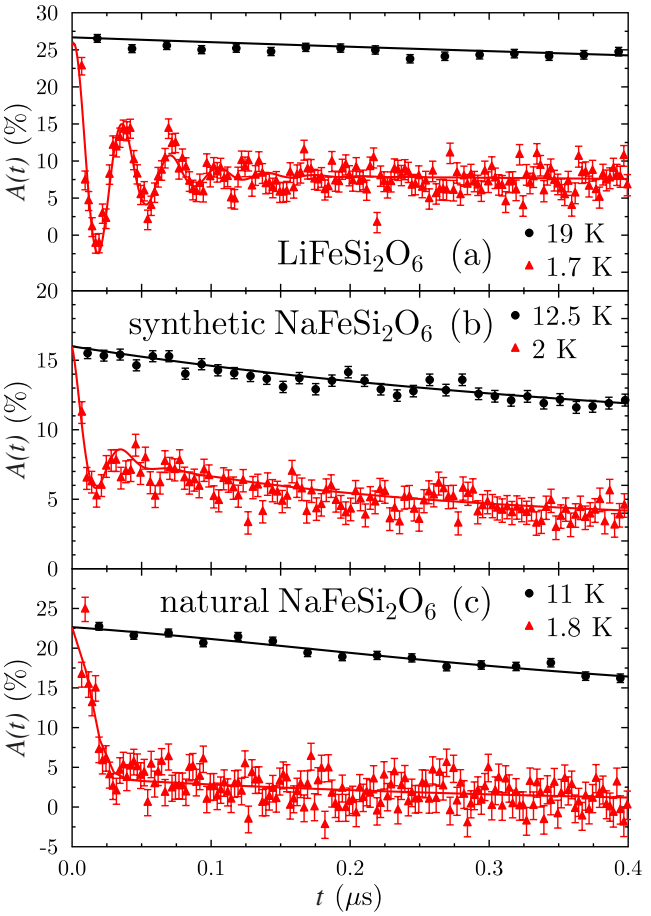

FIG. 3. (Color online) Muon asymmetry data above and below the magnetic transitions for (a) $LiFeSi_2O_6$, (b) synthetic $NaFeSi_2O_6$, and (c) natural $NaFeSi_2O_6$. Below T_N we fit with Eq. (1) for (a) and (b), and Eq. (2) for (c). Above T_N the relaxation is exponential. The widths of the time bins in the asymmetry histograms have been increased for clarity. For the synthetic $NaFeSi_2O_6$, measurements were done with the initial muon spin rotated differently relative to the detectors, leading to the lower asymmetry values.

The parameters extracted from the μSR data analysis are shown in Fig. 4. As shown in Fig. 4(a), the precession frequencies in $LiFeSi_2O_6$ and synthetic $NaFeSi_2O_6$ are well described by the phenomenological function: $\nu(T) = \nu(0)[1-(T/T_N)^\alpha]^\beta$. For $LiFeSi_2O_6$, $\nu(0) = 28.9(3)$ MHz, $T_N = 18.50(1)$ K, $\alpha = 1.6(2)$, and $\beta = 0.26(2)$. This implies that the $T \to 0$ internal field at the muon site is approximately 0.2 T. For synthetic $NaFeSi_2O_6$ the frequency is less well defined because the oscillations are far more strongly damped and, constraining α to the value found for the Li sample, we find $\nu(0) = 27(1)$ MHz, $T_N = 7.07(5)$ K, and $\beta = 0.28(4)$.

The data for natural $NaFeSi_2O_6$ show no coherent muon precession [see Fig. 3(c)], suggesting there is a large range of quasistatic fields at muon stopping sites. Such a distribution generally leads to a Kubo-Toyabe function,[26] which shows a dip and recovery in the asymmetry that is not evident in our data. Instead, we can effectively describe the measured asymmetry using a rapid Gaussian relaxation to describe the effect of the quasistatic fields and a slow exponential that

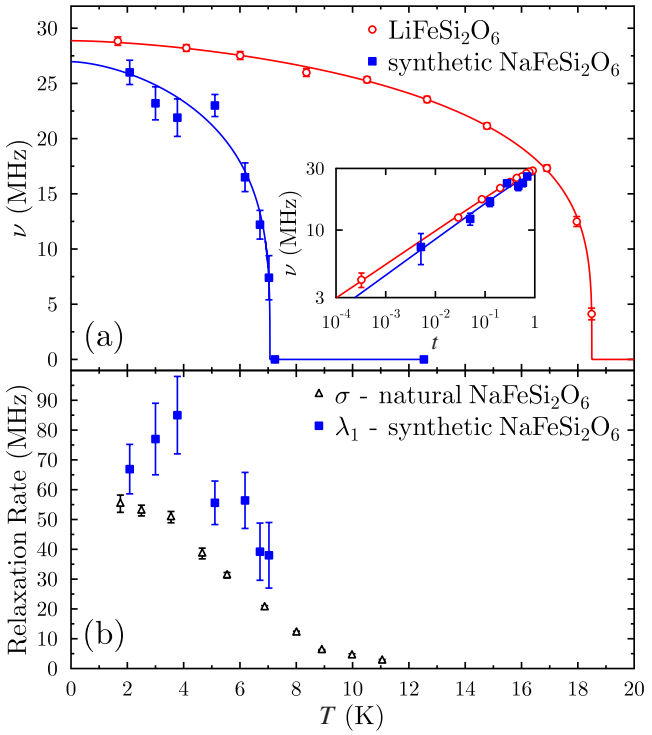

FIG. 4. (Color online) (a) Muon oscillation frequencies, ν [Eq. (1)], for $LiFeSi_2O_6$ and the synthetic sample of $NaFeSi_2O_6$ with fits described in the text. (Inset) The oscillation frequencies plotted against reduced temperature, $t=(T_N-T)/T_N$, showing the similarity of the trends approaching T_N. (b) The Gaussian relaxation rate, σ [Eq. (2)], for the natural $NaFeSi_2O_6$ and the linewidth λ_1 for the synthetic $NaFeSi_2O_6$.

describes the 1/3 tail expected for the Kubo-Toyabe function,

$$A(t) = A_1 e^{-\sigma^2 t^2} + A_2 e^{-\Lambda t}. \quad (2)$$

In analogy with Eq. (1) the first term describes incoherent muon precession about large static magnetic fields and the second term describes spin flipping of muons with their spin direction aligned along the local magnetic field by magnetic fluctuations. Because the experiment on natural $NaFeSi_2O_6$ was carried out on a large single crystal we have no expectation for the ratio $A_1:A_2$ because the details of the magnetic structure are unclear. Figure 4(b) presents the values of σ for natural $NaFeSi_2O_6$ and λ_1 for the synthetic sample. The relaxation rate σ does not follow the same power law as the precession frequencies, with a gradual growth through the two transitions observed previously,[12] suggesting that the intermediate phase may be obscured by the site disorder.

To compare the distributions of fields observed in the two $NaFeSi_2O_6$ samples we fitted the first 0.05 μs of the 2 K data sets to a Gaussian Kubo-Toyabe function[26] as this provides a consistent means of parametrizing these data, although worse in both cases than the functions used above. The widths of the field distributions coming from these fits were $\Delta_s=117(5)$ MHz$\sim$0.9 T for the synthetic sample and $\Delta_n=55(3)$ MHz$\sim$0.4 T for the natural sample. Such a difference could come from a change in the magnetic structure and/or the effects of Fe^{3+} dilution in the natural sample. To model this we need to find plausible muon stopping sites and calculate the effects of site dilution on the field distribution.

In order to find the muon stopping sites we calculated the dipole field distribution coming from Fe^{3+} moments within a radius of 20 unit cells for two plausible simple magnetic structures, ferromagnetic chains coupled antiferromagnetically, and antiferromagnetic chains coupled antiferromagnetically, with the moments aligned along the chain direction. The observed oscillation frequency is compatible in both cases with muons stopping near the oxygen atoms linking the Fe octahedra and Si tetrahedra, $\sim a/4$ from the Fe chains, preventing us from determining the magnetic structure on this basis.

To calculate the effect of the $\sim$17% of Fe^{3+} sites which are not occupied by Fe^{3+} ions [see Sec. II A] we made a simplified model assuming that all the impurities are nonmagnetic, homogeneously distributed, and only neighboring sites make significant contributions to the dipolar field experienced by the muon. Given the impurity concentration, $\sim$90% of muons will have 0, 1, or 2 impurities on neighboring sites so we only considered these possibilities. The distribution of fields was calculated by combining the dipolar fields with different missing neighbors with the probabilities appropriate for each combination. It is dominated by the effect of the closest iron moment to the muon site, which is around $\sim$0.35 T, but averaging over the neighboring sites leads to a distribution width $\Delta B\sim 0.25$ T. This is rather too small to be the sole contribution to the difference in the field distributions in the two $NaFeSi_2O_6$ samples but a change in the magnetic structure combined with the site dilution would be compatible with the difference observed.

III. DISCUSSION

In the inset to Fig. 4(a) we show the muon oscillation frequencies for the two synthetic samples plotted against reduced temperature, $t=(T_N-T)/T_N$. This shows the similarity of the critical behavior, intermediate between two and three dimensional. From the form of the muon data in each of the three samples we can infer certain aspects of the magnetic behavior. The coherent oscillations seen in $LiFeSi_2O_6$ are good evidence for commensurate magnetic ordering. The larger damping rate of the oscillations in synthetic $NaFeSi_2O_6$ could signal either a shorter magnetic coherence length or incommensuration. As is generally the case in magnetically induced multiferroics, the polar phase observed in natural $NaFeSi_2O_6$ is accessed from the paramagnetic phase via two second-order phase transitions.[19] In the synthetic sample only one transition is observed, so it appears unlikely that it is multiferroic. Considering the natural sample of $NaFeSi_2O_6$, there are no coherent oscillations and the change from the synthetic sample cannot be explained solely in terms of the effects of site dilution, as discussed above. A change from commensurate to incommensurate magnetic order may contribute to the difference but breaking up the intrachain ordering[27] or inducing a significant staggered magnetization around impurity sites[28] cannot be excluded from consideration.

We can also compare our results with those reported on the other quasi-one-dimensional multiferroics $LiCu_2O_2$ (Ref.

6) and $Ca_3(Co,Mn)_2O_6$.[7] The former is more analogous to natural $NaFeSi_2O_6$ since there are two closely spaced magnetic transitions bounding a magnetically but not ferroelectrically ordered intermediate phase. The heat capacity measurements suggest that $NaFeSi_2O_6$ is rather more one dimensional than $LiCu_2O_2$. Both of these compounds show considerable evidence for disorder influencing the multiferroic properties, due to Li nonstoichiometry in $LiCu_2O_2$ and on-chain site disorder in $Ca_3(Co,Mn)_2O_6$. However, unlike our natural sample, in both of these compounds oscillations in the muon decay asymmetry could be resolved at low temperature.[29,30]

In conclusion, we have used muon-spin relaxation and heat capacity measurements to probe the dimensionality and criticality in $LiFeSi_2O_6$ and $NaFeSi_2O_6$. Both synthetic samples show magnetic ordering that is apparently incompatible with multiferroicity. A natural sample of $NaFeSi_2O_6$, in which impurities occupy around 17% of the Fe^{3+} ion sites, shows significant effects of disorder yet is multiferroic. These results call for further study of the effect of disorder on multiferroicity and impurity effects in simpler quasi-one-dimensional magnets.

ACKNOWLEDGMENTS

Part of this work was performed at the Swiss Muon Source, Paul Scherrer Institute, Villigen, CH. We are grateful to Hubertus Luetkens for experimental assistance, Pierre Tolédano for helpful discussions, and to the EPSRC and STFC (U.K.) for financial support. This research project has been supported by the European Commission under the Seventh Framework Programme through the 'Research Infrastructures' action of the 'Capacities' Programme, Contract No CP-CSA_INFRA-2008-1.1.1 Number 226507-NMI3.

*peter.baker@stfc.ac.uk

[1] M. Fiebig, J. Phys. D **38**, R123 (2005).
[2] Y. Tokura, Science **312**, 1481 (2006).
[3] W. Eerenstein, N. D. Mathur, and J. F. Scott, Nature (London) **442**, 759 (2006).
[4] T. Kimura, T. Goto, H. Shintani, K. Ishizaka, T. Arima, and Y. Tokura, Nature (London) **426**, 55 (2003).
[5] N. Hur, S. Park, P. A. Sharma, J. S. Ahn, S. Guha, and S.-W. Cheong, Nature (London) **429**, 392 (2004).
[6] A. Rusydi *et al.*, Appl. Phys. Lett. **92**, 262506 (2008).
[7] Y. J. Choi, H. T. Yi, S. Lee, Q. Huang, V. Kiryukhin, and S.-W. Cheong, Phys. Rev. Lett. **100**, 047601 (2008).
[8] M. Mostovoy, Phys. Rev. Lett. **96**, 067601 (2006).
[9] J. J. Betouras, G. Giovannetti, and J. van den Brink, Phys. Rev. Lett. **98**, 257602 (2007).
[10] T. Kimura, G. Lawes, T. Goto, Y. Tokura, and A. P. Ramirez, Phys. Rev. B **71**, 224425 (2005).
[11] S. Lee *et al.*, Nature (London) **451**, 805 (2008).
[12] S. Jodlauk, P. Becker, J. A. Mydosh, D. I. Khomskii, T. Lorenz, S. V. Streltsov, D. C. Hezel, and L. Bohatý, J. Phys.: Condens. Matter **19**, 432201 (2007).
[13] G. J. Redhammer and G. Roth, Z. Kristallogr. **219**, 278 (2004).
[14] M. Isobe, E. Ninomiya, A. N. Vasil'ev, and Y. Ueda, J. Phys. Soc. Jpn. **71**, 1423 (2002).
[15] P. J. Baker *et al.*, Phys. Rev. B **75**, 094404 (2007).
[16] G. J. Redhammer, G. Roth, W. Treutmann, M. Hoelzel, W. Paulus, G. André, C. Pietzonka, and G. Amthauer, J. Solid State Chem. **182**, 2374 (2009).
[17] G. Nénert, M. Isobe, C. Ritter, O. Isnard, A. N. Vasiliev, and Y. Ueda, Phys. Rev. B **79**, 064416 (2009).
[18] O. Ballet, J. M. D. Coey, G. Fillion, A. Ghose, A. Hewat, and J. R. Regnard, Phys. Chem. Miner. **16**, 672 (1989).
[19] B. Mettout, P. Tolédano, and M. Fiebig (unpublished).
[20] S. V. Streltsov and D. I. Khomskii, Phys. Rev. B **77**, 064405 (2008).
[21] L. J. de Jongh and A. R. Miedema, Adv. Phys. **23**, 1 (1974).
[22] M. Zhang, G. J. Redhammer, E. K. H. Salje, and M. Mookherjee, Phys. Chem. Miner. **29**, 609 (2002).
[23] H. C. Ko, M. J. Ferrante, and J. M. Stuve, Proceedings of the Seventh Symposium on Thermophysical Properties (American Society of Mechanical Engineers, New York, 1977), p. 392.
[24] S. J. Blundell, Contemp. Phys. **40**, 175 (1999).
[25] F. L. Pratt, Physica B **289-290**, 710 (2000).
[26] R. S. Hayano, Y. J. Uemura, J. Imazato, N. Nishida, T. Yamazaki, and R. Kubo, Phys. Rev. B **20**, 850 (1979).
[27] Y. Imry, P. A. Montano, and D. Hone, Phys. Rev. B **12**, 253 (1975).
[28] S. Eggert and I. Affleck, Phys. Rev. Lett. **75**, 934 (1995).
[29] B. Roessli, U. Staub, A. Amato, D. Herlach, P. Pattison, K. Sablina, and G. A. Petrakovskii, Physica B **296**, 306 (2001).
[30] T. Lancaster, S. J. Blundell, P. J. Baker, H. J. Lewtas, W. Hayes, F. L. Pratt, H. T. Yi, and S.-W. Cheong, Phys. Rev. B **80**, 020409(R) (2009).